

# Similarities and Differences in the Fermiology of Kagome Metals $AV_3Sb_5$ (A=K, Rb, Cs) Revealed by Shubnikov-de Haas Oscillations

Zheyu Wang<sup>§,1</sup> Wei Zhang<sup>§,1</sup> Lingfei Wang,<sup>1</sup> Tsz Fung Poon,<sup>1</sup> Chun Wai Tsang,<sup>1</sup> Wenyan Wang,<sup>1</sup> Jianyu Xie,<sup>1</sup> Xuefeng Zhou,<sup>2</sup> Yusheng Zhao,<sup>2</sup> Shanmin Wang,<sup>2</sup> Ming-zhong Ai,<sup>1</sup> Kwing To Lai,<sup>1,3</sup> and Swee K. Goh<sup>1,\*</sup>

<sup>1</sup>*Department of Physics, The Chinese University of Hong Kong, Shatin, Hong Kong, China*

<sup>2</sup>*Department of Physics, Southern University of Science and Technology, Shenzhen, Guangdong, China*

<sup>3</sup>*Shenzhen Research Institute, The Chinese University of Hong Kong, Shatin, Hong Kong, China*

(Dated: April 4, 2023)

Materials with  $AV_3Sb_5$  (A=K, Rb, Cs) stoichiometry are recently discovered kagome superconductors with the electronic structure featuring a Dirac band, van Hove singularities and flat bands. These systems undergo anomalous charge-density-wave (CDW) transitions at  $T_{CDW} \sim 80 - 100$  K, resulting in the reconstruction of the Fermi surface from the pristine phase. Although comprehensive investigations of the electronic structure via quantum oscillations (QOs) have been performed on the sister compounds  $CsV_3Sb_5$  and  $RbV_3Sb_5$ , a detailed QO study of  $KV_3Sb_5$  is so far absent. Here, we report the Shubnikov-de Haas QO study in  $KV_3Sb_5$ . We resolve a large number of new frequencies with the highest frequency of 2202 T (occupying  $\sim 54\%$  of the Brillouin zone area in the  $k_x$ - $k_y$  plane). The Lifshitz-Kosevich analysis further gives relatively small cyclotron effective masses, and the angular dependence study reveals the two-dimensional nature of the frequencies with a sufficient signal-to-noise ratio. Finally, we compare the QO spectra for all three  $AV_3Sb_5$  compounds collected under the same conditions, enabling us to point out the similarities and differences across these systems. Our results fill in the gap of the QO study in  $KV_3Sb_5$  and provide valuable data to understand the band structure of all three members of  $AV_3Sb_5$ .

## I. INTRODUCTION

The kagome metals  $AV_3Sb_5$  (A=K, Rb, Cs) with vanadium atoms arranged in a perfect kagome net configuration host flat electronic bands, van Hove singularities and Dirac points [1–5]. As such, these systems offer an ideal platform to explore the interplay between the band topology and electronic correlation [6–8]. Interestingly, these metals enter anomalous charge-density-wave (CDW) phases ( $T_{CDW} \sim 80 - 100$  K) and exhibit superconductivity ( $T_c \sim 0.9 - 2.7$  K) on cooling [3–5, 9–17]. The CDW order and superconductivity exhibit an interesting interplay, as revealed by high-pressure experiments [18–21]. Besides, recent studies detected the time-reversal symmetry breaking and electronic nematicity in the CDW phase, evoking extensive exploration of the possible unconventional superconductivity (SC) in  $AV_3Sb_5$  [22–28].

Although all three members of  $AV_3Sb_5$  take the same crystal structure in the pristine phase, both the superconducting and the CDW states exhibit crucial differences. Apart from the obvious difference in  $T_c$ , the superconducting gap and its behaviour against pressure are different. For  $KV_3Sb_5$  and  $RbV_3Sb_5$ , the superconducting gap has been reported to be nodal at ambient pressure, but as pressure increases the gap becomes nodeless [29]. For  $CsV_3Sb_5$ , accumulating evidence points to the nodeless gap at ambient pressure, and the application of pressure does not affect the nodeless nature of the superconducting gap [30–36]. Concerning the CDW state,

important differences have also been noted. In the CDW state of  $CsV_3Sb_5$ , a complicated superlattice involving the stacking of “Star of David” (SoD) and trihexagonal (TrH) in-plane distortions has been proposed, quadrupling the periodicity along the  $c$ -axis (such a distortion is denoted as “ $2 \times 2 \times 4$ ”) [5, 37]. On the other hand, the charge order in  $KV_3Sb_5$  and  $RbV_3Sb_5$  adopt a staggered TrH configuration with a  $\pi$  shift between the adjacent layers, resulting in a  $2 \times 2 \times 2$  distortion [5]. Given that the SC phase arises from the CDW state, as  $T_c < T_{CDW}$  for all three systems, it is important to understand the normal state in the presence of the CDW for an eventual understanding of the superconductivity.

The CDW order unavoidably plays an important role on the Fermiology of these kagome metals. From the scanning tunnelling microscopy (STM) and angle-resolved photoemission spectroscopy (ARPES) measurements, an energy gap opens near the Fermi level during the CDW transition and the Fermi surfaces are reconstructed [5, 9, 38–40]. Due to the complicated CDW order, the Fermi surface in the CDW phase can be very different from the pristine phase. Quantum oscillations (QOs) have been most heavily studied in the CDW phase of  $CsV_3Sb_5$ , revealing rich QO spectra with frequencies up to 9930 T [18, 37, 41–47]. Surprisingly, a significantly simpler QO spectrum was reported in  $KV_3Sb_5$  – only two low frequencies (34.6 T and 148.9 T) were revealed by the Shubnikov-de Haas (SdH) effect in the pioneering work of  $KV_3Sb_5$  [48]. Interestingly, a simple QO spectrum with only two small frequencies was also initially reported in  $RbV_3Sb_5$ , but a later study by some of us uncovered a much richer spectrum with the largest maximum QO frequency extending beyond 2000 T [49, 50]. Therefore, it is a pressing issue to revisit the Fermiology of  $KV_3Sb_5$

\* skgoh@cuhk.edu.hk

via QOs.

In this work, we measure the SdH quantum oscillations using high-quality single crystals of  $\text{KV}_3\text{Sb}_5$ . We resolve a large number of new frequencies with the highest frequency of 2202 T. This frequency is significant, as it represents  $\sim 54\%$  of the reconstructed Brillouin zone area in the  $k_x$ - $k_y$  plane. The Lifshitz-Kosevich analysis further gives relatively small cyclotron effective masses, and the angular dependence study reveals the two-dimensional nature for the frequencies with a sufficient signal-to-noise ratio. Our results show that the QO spectra in all three compounds are complicated, likely resulting from the complex CDW order, and that large Fermi surfaces beyond the expectation from the initial QO reports exist in these metals.

## II. METHODS

Single crystals of  $\text{KV}_3\text{Sb}_5$  were synthesized from K (ingot, 99.97%), V (powder, 99.9%), and Sb (shot, 99.9999%), using self-flux method similar to Ref. [1]. Raw materials with the molar ratio of K:V:Sb = 5:3:14 were sealed in a stainless steel jacket in an argon-filled glovebox and then moved to the furnace for heat treatment. The mixture was first heated to 1000 °C at the rate of 20 °C/h. After being held at 1000 °C for 24 h, it was cooled to 900 °C at 50 °C/h, followed by a further cooling to 400 °C at 2 °C/h. The as-grown single crystals were millimeter-sized shiny plates. X-ray diffraction measurements were performed at room temperature by using a Rigaku X-ray diffractometer with  $\text{CuK}\alpha$  radiation. The chemical compositions were characterized by a JEOL JSM-7800F scanning electron microscope equipped with an Oxford energy-dispersive X-ray (EDX) spectrometer.

Magnetotransport measurements were conducted in a Physical Property Measurement System by Quantum Design. For bulk crystals, the electrical contacts were prepared with gold wires and silver paste while for thin flakes, the samples were first exfoliated from bulk crystals and then transferred onto a diamond substrate pre-patterned with conducting electrodes [49, 51–53]. The thin flake sample was encapsulated by a h-BN film to avoid oxidization. All operations above were conducted in an argon-filled glovebox. The total thickness of h-BN encapsulated flake was determined by a Bruker BioScope Resolve atomic force microscope (AFM). The thickness of h-BN is determined separately. The flake thickness is then the difference between the two AFM measurements. A Stanford Research 830 lock-in amplifier was used for Shubnikov-de Haas effect measurements. The rotator insert option by Quantum Design was used to tilt the angle between magnetic field and the sample. During the rotation, the current direction is kept perpendicular to the magnetic field.

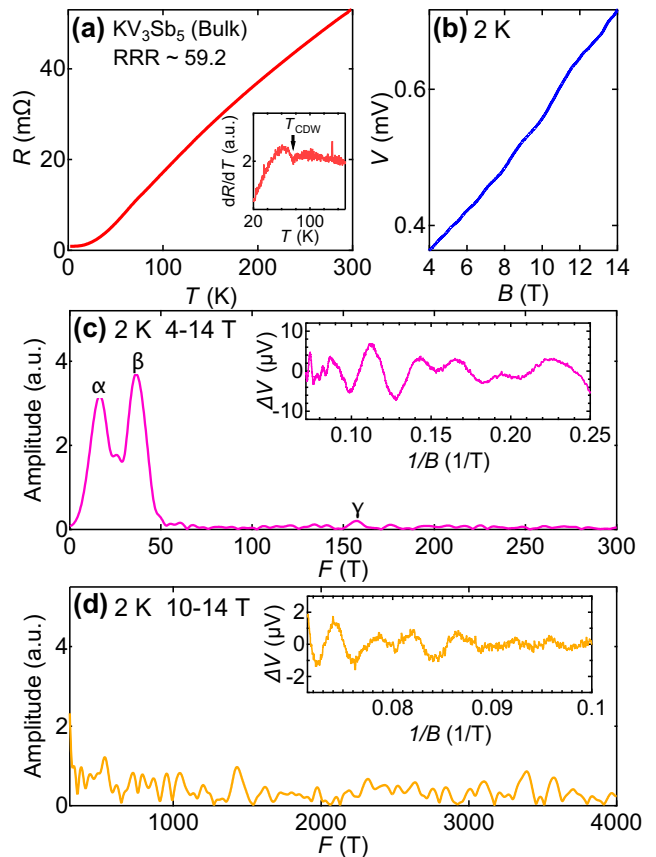


FIG. 1. (a) Temperature dependence of resistance for a bulk  $\text{KV}_3\text{Sb}_5$  sample. The RRR is 59.2. The inset is the temperature dependence of  $dR/dT$ , showing the determination of  $T_{\text{CDW}}$ . (b) Raw data of the lock-in voltage against the magnetic field at 2 K with  $B \parallel c$ . FFT spectra of the bulk sample for the oscillation data from (c) 4 T to 14 T and (d) 10 T to 14 T. The insets show the oscillatory signals after removing the background.

## III. RESULTS

Figure 1(a) shows the temperature dependence of resistance,  $R(T)$ , in a bulk  $\text{KV}_3\text{Sb}_5$  sample. The residual resistivity ratio (RRR, defined as  $\rho(300 \text{ K})/\rho(2 \text{ K})$ ) is 59.2, which is the highest among the reported values, indicating the high quality of our sample. On cooling, there is a weak anomaly in  $R(T)$  and correspondingly, a dip feature appears in the  $dR/dT$  curve at around 78 K (inset of Fig. 1(a)), which is consistent with the reported CDW transition [19, 39, 48].

The high purity of the sample enables us to study the SdH effect in  $\text{KV}_3\text{Sb}_5$ . As shown in Fig. 1(b), the SdH quantum oscillation signals can be recognized in the field-dependent resistive signals even without removing the background. We further perform the fast Fourier transformation (FFT) analysis. As displayed in Fig. 1(c), apart from  $\beta$  (35 T) and  $\gamma$  (157 T), which have been

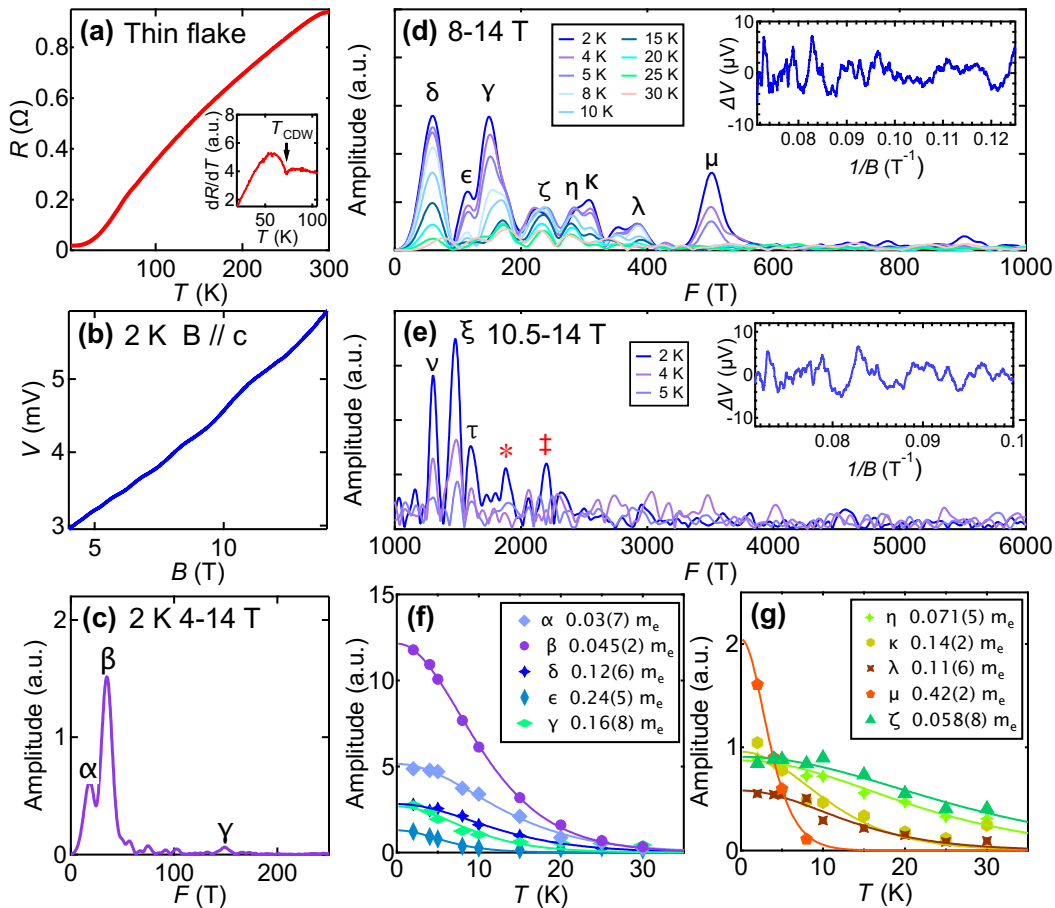


FIG. 2. (a) Temperature dependence of the resistance for a thin flake of  $\text{KV}_3\text{Sb}_5$ . The inset is the temperature dependence of  $dR/dT$ , allowing the determination of  $T_{\text{CDW}}$ . (b) Resistive voltage against the magnetic field at 2 K with  $B \parallel c$ . FFT spectra of the thin flake for the oscillation data from (c) 4 T to 14 T, (d) 8 T to 14 T and (e) 10.5 T to 14 T. For the peaks labelled by “\*” and “†”, we only observed them at 2 K. The insets in (d) and (e) show the oscillation signals with the background subtracted. (f), (g) Temperature dependence of oscillation amplitudes. The symbols are experimental data and the solid curves are the Lifshitz-Kosevich fits.

revealed by previous study [48], we resolve another new QO frequency ( $F_\alpha = 16$  T). When a shorter field range (between 10 T and 14 T) is used, which would preferentially enhance the spectral intensities of relatively high QO frequencies, we do not observe conclusive peaks in the FFT spectrum (Fig. 1(d)).

Previous QO studies on the sister compounds  $\text{RbV}_3\text{Sb}_5$  and  $\text{CsV}_3\text{Sb}_5$  have uncovered much higher QO frequencies. To search for higher frequencies in  $\text{AV}_3\text{Sb}_5$ , it is necessary to improve the signal-to-noise ratio. One avenue would be to extend the maximum field of the experiment, as was adopted by the authors of Refs. [41, 44, 45] on  $\text{CsV}_3\text{Sb}_5$ . Here, we choose to enhance the resistive signal strength by optimizing the sample geometry – we prepare a device using a 80-nm-thick flake of  $\text{KV}_3\text{Sb}_5$  exfoliated from the bulk crystal. Figures 2(a) and 2(b) show the temperature- and field-dependence of the resistive signals in the thin flake of  $\text{KV}_3\text{Sb}_5$ , respectively. The magnetic field is applied along the sample

$c$ -axis. Analyzing the signals carefully, we uncover a rich QO spectrum. As displayed in Fig. 2(c),  $F_\alpha$  (18 T),  $F_\beta$  (35 T) and  $F_\gamma$  (148 T) are resolved using a long field range of 4 – 14 T, consistent with the results of the bulk sample (*c.f.* Fig. 1(c)). However, new frequencies can be readily observed when narrower field windows are employed, as displayed in Figs. 2(d) and (e). Figure 2(d) shows the FFT spectrum with the field range of 8 – 14 T and we resolve  $F_\delta = 60$  T,  $F_\epsilon = 115$  T,  $F_\zeta = 237$  T,  $F_\eta = 285$  T,  $F_\kappa = 308$  T,  $F_\lambda = 385$  T and  $F_\mu = 502$  T below 1000 T. In Fig. 2(e) in which a field window of 10.5 – 14 T is used, much higher frequencies can be seen:  $F_\nu = 1304$  T,  $F_\xi = 1480$  T,  $F_\tau = 1601$  T and probably  $F_* = 1879$  T, and  $F_\ddagger = 2202$  T. For  $F_*$  and  $F_\ddagger$ , the oscillatory signals already fade away at 4 K, rendering their presence more uncertain.

We next measure QOs at different temperatures and we carefully trace the temperature dependence of the QO amplitudes for ten frequencies, enabling the deter-

mination of cyclotron effective masses. As displayed in Figs. 2(f) and 2(g), the cyclotron effective masses obtained by the Lifshitz-Kosevich (LK) analysis are small, with the values  $\sim 0.1 m_e$  or below, except for  $m_e = 0.24 m_e$  and  $m_\mu = 0.42 m_e$ . The small effective masses indicate that these frequencies originate from electronic bands with quasilinear nature. Unfortunately, we are unable to determine the effective masses for the peaks larger than 1300 T, as the QO amplitudes decrease rapidly at higher temperatures (see Fig. 2(e)). Based on the effective masses we are able to extract, the rather low effective masses are consistent with the sister kagome compound  $\text{CsV}_3\text{Sb}_5$  and  $\text{RbV}_3\text{Sb}_5$  [37, 47, 49, 53].

We now explore the dimensionality of the Fermi surfaces by measuring SdH oscillations at various magnetic field angles. Here  $\theta = 0$  refers to  $B \parallel c$  and the rotation is towards the  $ab$  plane. Due to the difference in the amplitudes, FFT spectra are magnified by different factors, and they are divided into three frequency ranges for visual clarity, see Figs. 3(a) – 3(c). When  $\theta$  increases, all frequencies shift to higher values and the intensities gradually decrease. Peaks at lower frequencies ( $F_\beta$  and  $F_\gamma$ ) can be tracked up to  $40^\circ$  while  $F_\zeta$ ,  $F_\kappa$  and  $F_\mu$ , which are less intense, disappear at around  $20^\circ$ . The angular dependence of these frequencies are displayed in Figs. 3(d) and 3(e) and are well-described by the formula  $F(\theta) = F(0^\circ)/\cos(\theta)$ , consistent with the two-dimensional feature of Fermi surfaces. Thus, the angular dependence results in  $\text{KV}_3\text{Sb}_5$  are similar to the results in both  $\text{RbV}_3\text{Sb}_5$  and  $\text{CsV}_3\text{Sb}_5$  [37, 42, 49, 53] and consistent with the two-dimensional nature of Fermi surfaces obtained by density functional theory (DFT) calculations of  $\text{KV}_3\text{Sb}_5$  [12, 54].

#### IV. DISCUSSION

The complex SdH spectrum of  $\text{KV}_3\text{Sb}_5$ , which features QO frequencies spanning a large range, is reminiscent of the spectra observed in the sister compounds  $\text{RbV}_3\text{Sb}_5$  and  $\text{CsV}_3\text{Sb}_5$ . Given that some of us have recently studied QOs in both  $\text{RbV}_3\text{Sb}_5$  [49] and  $\text{CsV}_3\text{Sb}_5$  [53] with the same experimental protocol, it is meaningful to compare our data across all three kagome metals  $\text{AV}_3\text{Sb}_5$ . Figure 4 summarizes the SdH spectra of  $\text{KV}_3\text{Sb}_5$ ,  $\text{RbV}_3\text{Sb}_5$  and  $\text{CsV}_3\text{Sb}_5$  at 2 K and with  $B \parallel c$ . To display the spectra in different frequency regions, the field window for performing the FFT has been carefully chosen and applied consistently across three systems.

Figures 4(a), 4(b) and 4(c) respectively show the low-frequency spectra of  $\text{KV}_3\text{Sb}_5$ ,  $\text{RbV}_3\text{Sb}_5$  and  $\text{CsV}_3\text{Sb}_5$ , with the field range of 4 – 14 T. Similar double-peak structure located below 50 T can be seen, in addition to another peak whose frequency decreases systematically when the atomic size of the alkali element increases: in  $\text{KV}_3\text{Sb}_5$ ,  $\text{RbV}_3\text{Sb}_5$  and  $\text{CsV}_3\text{Sb}_5$ , the frequency is 149 T, 124 T and 72 T, respectively. According to previous studies [42], the 72 T peak in  $\text{CsV}_3\text{Sb}_5$  corresponds to a small

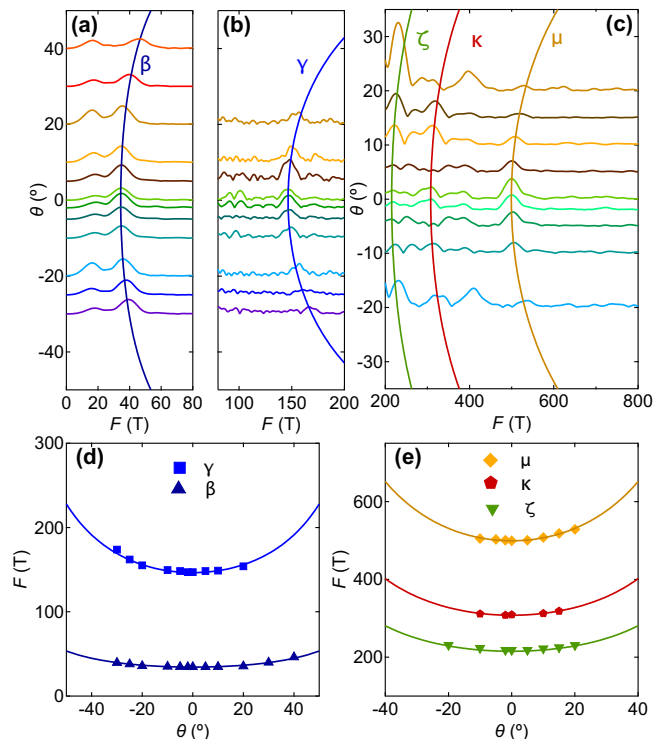


FIG. 3. FFT spectra at different field angles for the frequency range of (a) 0 to 80 T, (b) 80 to 200T, (c) 200 to 800 T. (d, e) Angular dependence of QO frequencies. The solid curves are fits using  $F(\theta) = F(0^\circ)/\cos(\theta)$ .

oval-shaped pocket near the L point in the first Brillouin zone. In  $\text{KV}_3\text{Sb}_5$ , a similar oval-shaped pocket was also reported near the L point in DFT calculations [39] and this could be assigned to the 149 T peak we detected.

To have a better view of the higher frequencies, narrower field windows have been used, resulting in the spectra displayed in Figs. 4(d)–4(i). Although the signal-to-noise ratios are different, similar features can be spotted: oscillation frequencies near 2200 T and around 1400 T, as shown in Figs. 4(g), 4(h) and 4(i). We note that the frequencies over 2000 T in Fig. 4(i) are beyond the expectation in DFT calculations taking into account a  $2 \times 2 \times 4$  distortion of  $\text{CsV}_3\text{Sb}_5$  [53], and their presence has been linked to orbital-selective charge doping. Meanwhile, the QO spectra of  $\text{KV}_3\text{Sb}_5$  and  $\text{RbV}_3\text{Sb}_5$  also contain frequencies beyond 2000 T, although they are less intense than the  $\text{CsV}_3\text{Sb}_5$  counterpart. Hence, further studies are needed to settle the origin of these high-frequency peaks. Finally, prominent differences appear in the mid-frequency range, see Figs. 4(d)–4(f). Contrary to  $\text{CsV}_3\text{Sb}_5$ , in which multiple frequencies with nearly equal spacing appear between 400 T to 1000 T, both  $\text{KV}_3\text{Sb}_5$  and  $\text{RbV}_3\text{Sb}_5$  show simpler spectra with better-defined, relatively more isolated peaks.

At the qualitative level, the QO spectrum of  $\text{KV}_3\text{Sb}_5$  resembles the spectrum of  $\text{RbV}_3\text{Sb}_5$  more than that of

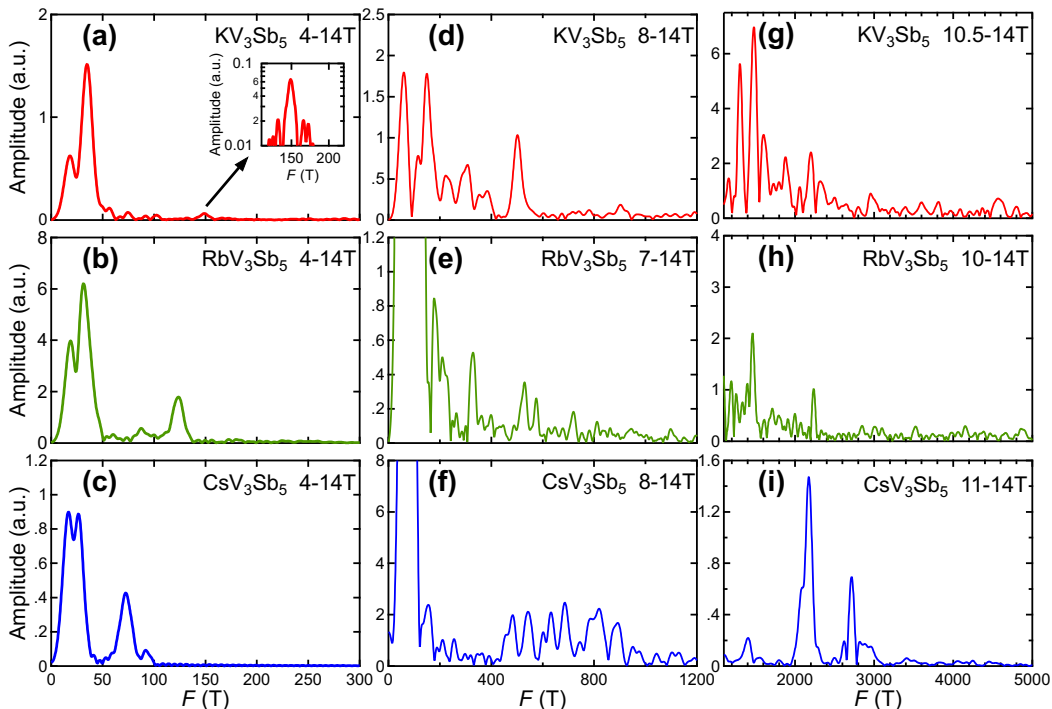


FIG. 4. Comparison of SdH oscillation spectra of  $KV_3Sb_5$ ,  $RbV_3Sb_5$  and  $CsV_3Sb_5$ . (a-c) The FFT spectra from 0 T to 300 T, (d-f) the FFT spectra from 0 to 1200 T and (g-i) the FFT spectra from 1100 T to 5000 T. Different field windows for performing FFT were used for different frequency ranges. The inset in (a) offers a better view of  $F_\gamma$  in  $KV_3Sb_5$ . Data of  $RbV_3Sb_5$  and  $CsV_3Sb_5$  come from Ref. [49] and Ref. [53], respectively.

$CsV_3Sb_5$ . This could reflect the differences in the CDW distortion. In  $KV_3Sb_5$  and  $RbV_3Sb_5$ , a  $2 \times 2 \times 2$  distortion has been reported [5], while  $CsV_3Sb_5$  adopts a more complicated  $2 \times 2 \times 4$  distortion [5, 37] - the mid-frequency and the high-frequency spectra could be more sensitive to the precise nature of the CDW distortion. Nevertheless, all three kagome metals display rich QO spectra with recognizable similarity, quasi-2D Fermi surfaces as well as light effective masses.

## V. CONCLUSIONS

In summary, we have conducted the SdH quantum oscillation measurements in high-quality single crystals of  $KV_3Sb_5$ . We resolve a large number of new frequencies up to 2202 T. The Lifshitz-Kosevich analysis reveals relatively small cyclotron effective masses and the angular dependence of the QO frequencies are consistent with two-dimensional Fermi surfaces. We further compare the

QO spectra for all three kagome metals  $AV_3Sb_5$ . Our results show that the QO spectra in all three compounds are complicated because of the complex CDW order, and that large Fermi surfaces exist in these metals. Our results fill in the gap of the QO study in  $KV_3Sb_5$  and provide valuable data to understand the band structure of all three members of  $AV_3Sb_5$ .

## ACKNOWLEDGMENTS

We acknowledge support by Research Grants Council of Hong Kong (CUHK 14301020, CUHK 14300722, A-CUHK402/19), CUHK Direct Grant (4053461, 4053408, 4053528, 4053463), the National Natural Science Foundation of China (12104384, 12174175) and the Shenzhen Basic Research Fund (JCYJ20190809173213150).

<sup>§</sup>W.Z. and Z.W. contributed equally to this work.

[1] B. R. Ortiz, L. C. Gomes, J. R. Morey, M. Winiarski, M. Bordelon, J. S. Mangum, I. W. H. Oswald, J. A. Rodriguez-Rivera, J. R. Neilson, S. D. Wilson,

E. Ertekin, T. M. McQueen, and E. S. Toberer, “New kagome prototype materials: discovery of  $KV_3Sb_5$ ,  $RbV_3Sb_5$ , and  $CsV_3Sb_5$ ,” *Phys. Rev. Mater.* **3**, 094407

- (2019).
- [2] T. Neupert, M. M. Denner, J.-X. Yin, R. Thomale, and M. Z. Hasan, “Charge order and superconductivity in kagome materials,” *Nat. Phys.* **18**, 137 (2021).
  - [3] H. Li, T. T. Zhang, T. Yilmaz, Y. Y. Pai, C. E. Marvinney, A. Said, Q. W. Yin, C. S. Gong, Z. J. Tu, E. Vescovo, C. S. Nelson, R. G. Moore, S. Murakami, H. C. Lei, H. N. Lee, B. J. Lawrie, and H. Miao, “Observation of unconventional charge density wave without acoustic phonon anomaly in kagome superconductors  $AV_3Sb_5$  ( $A = Rb, Cs$ ),” *Phys. Rev. X* **11**, 031050 (2021).
  - [4] Z. Liu, N. Zhao, Q. Yin, C. Gong, Z. Tu, M. Li, W. Song, Z. Liu, D. Shen, Y. Huang, K. Liu, H. Lei, and S. Wang, “Charge-density-wave-induced bands renormalization and energy gaps in a kagome superconductor  $RbV_3Sb_5$ ,” *Phys. Rev. X* **11**, 041010 (2021).
  - [5] M. Kang, S. Fang, J. Yoo, B. R. Ortiz, Y. M. Oey, J. Choi, S. H. Ryu, J. Kim, C. Jozwiak, A. Bostwick, E. Rotenberg, E. Kaxiras, J. G. Checkelsky, S. D. Wilson, J.-H. Park, and R. Comin, “Charge order landscape and competition with superconductivity in kagome metals,” *Nature Mater.* **22**, 186 (2022).
  - [6] M. L. Kiesel and R. Thomale, “Sublattice interference in the kagome Hubbard model,” *Phys. Rev. B* **86**, 121105 (2012).
  - [7] M. L. Kiesel, C. Platt, and R. Thomale, “Unconventional Fermi surface instabilities in the kagome Hubbard model,” *Phys. Rev. Lett.* **110**, 126405 (2013).
  - [8] W.-S. Wang, Z.-Z. Li, Y.-Y. Xiang, and Q.-H. Wang, “Competing electronic orders on kagome lattices at van Hove filling,” *Phys. Rev. B* **87**, 115135 (2013).
  - [9] Z. Liang, X. Hou, F. Zhang, W. Ma, P. Wu, Z. Zhang, F. Yu, J.-J. Ying, K. Jiang, L. Shan, Z. Wang, and X.-H. Chen, “Three-dimensional charge density wave and surface-dependent vortex-core states in a kagome superconductor  $CsV_3Sb_5$ ,” *Phys. Rev. X* **11**, 031026 (2021).
  - [10] H. Zhao, H. Li, B. R. Ortiz, S. M. L. Teicher, T. Park, M. Ye, Z. Wang, L. Balents, S. D. Wilson, and I. Zeljkovic, “Cascade of correlated electron states in the kagome superconductor  $CsV_3Sb_5$ ,” *Nature* **599**, 216 (2021).
  - [11] Y. Hu, S. M. L. Teicher, B. R. Ortiz, Y. Luo, S. Peng, L. Huai, J. Z. Ma, N. C. Plumb, S. D. Wilson, J. F. He, and M. Shi, “Charge-order-assisted topological surface states and flat bands in the kagome superconductor  $CsV_3Sb_5$ ,” *Sci. Bull.* **67**, 495 (2022).
  - [12] E. Uykur, B. R. Ortiz, S. D. Wilson, M. Dressel, and A. A. Tsirlin, “Optical detection of charge-density-wave instability in the non-magnetic kagome metal  $KV_3Sb_5$ ,” *npj Quant. Mater.* **7**, 16 (2022).
  - [13] X. Zhou, Y. Li, X. Fan, J. Hao, Y. Dai, Z. Wang, Y. Yao, and H.-H. Wen, “Origin of charge density wave in the kagome metal  $CsV_3Sb_5$  as revealed by optical spectroscopy,” *Phys. Rev. B* **104**, L041101 (2021).
  - [14] Y.-X. Jiang, J.-X. Yin, M. M. Denner, N. Shumiya, B. R. Ortiz, G. Xu, Z. Guguchia, J. He, M. S. Hossain, X. Liu, J. Ruff, L. Kautzsch, S. S. Zhang, G. Chang, I. Belopolski, Q. Zhang, T. A. Cochran, D. Multer, M. Litskevich, Z.-J. Cheng, X. P. Yang, Z. Wang, R. Thomale, T. Neupert, S. D. Wilson, and M. Z. Hasan, “Unconventional chiral charge order in kagome superconductor  $KV_3Sb_5$ ,” *Nat. Mater.* **20**, 1353 (2021).
  - [15] S. Wu, B. R. Ortiz, H. Tan, S. D. Wilson, B. Yan, T. Birol, and G. Blumberg, “Charge density wave order in the kagome metal  $AV_3Sb_5$  ( $A = Cs, Rb, K$ ),” *Phys. Rev. B* **105**, 155106 (2022).
  - [16] R. Lou, A. Fedorov, Q. Yin, A. Kuibarov, Z. Tu, C. Gong, E. F. Schwier, B. Büchner, H. Lei, and S. Borisenko, “Charge-density-wave-induced peak-dip-hump structure and the multiband superconductivity in a kagome superconductor  $CsV_3Sb_5$ ,” *Phys. Rev. Lett.* **128**, 036402 (2022).
  - [17] T. Kato, Y. Li, M. Liu, K. Nakayama, Z. Wang, S. Souma, M. Kitamura, K. Horiba, H. Kumigashira, T. Takahashi, Y. Yao, and T. Sato, “Surface-termination-dependent electronic states in kagome superconductors  $AV_3Sb_5$  ( $A = K, Rb, Cs$ ) studied by micro-ARPES,” arXiv:2301.12034 (2023).
  - [18] F. Yu, D. Ma, W. Zhuo, S. Liu, X. Wen, B. Lei, J. Ying, and X. Chen, “Unusual competition of superconductivity and charge-density-wave state in a compressed topological kagome metal,” *Nat. Commun.* **12**, 3645 (2021).
  - [19] F. Du, S. Luo, B. R. Ortiz, Y. Chen, W. Duan, D. Zhang, X. Lu, S. D. Wilson, Y. Song, and H. Yuan, “Pressure-induced double superconducting domes and charge instability in the kagome metal  $KV_3Sb_5$ ,” *Phys. Rev. B* **103**, L220504 (2021).
  - [20] K. Y. Chen, N. N. Wang, Q. W. Yin, Y. H. Gu, K. Jiang, Z. J. Tu, C. S. Gong, Y. Uwatoko, J. P. Sun, H. C. Lei, J. P. Hu, and J.-G. Cheng, “Double superconducting dome and triple enhancement of  $T_c$  in the kagome superconductor  $CsV_3Sb_5$  under high pressure,” *Phys. Rev. Lett.* **126**, 247001 (2021).
  - [21] N. N. Wang, K. Y. Chen, Q. W. Yin, Y. N. N. Ma, B. Y. Pan, X. Yang, X. Y. Ji, S. L. Wu, P. F. Shan, S. X. Xu, Z. J. Tu, C. S. Gong, G. T. Liu, G. Li, Y. Uwatoko, X. L. Dong, H. C. Lei, J. P. Sun, and J.-G. Cheng, “Competition between charge-density-wave and superconductivity in the kagome metal  $RbV_3Sb_5$ ,” *Phys. Rev. Res.* **3**, 043018 (2021).
  - [22] L. Yu, C. Wang, Y. Zhang, M. Sander, S. Ni, Z. Lu, S. Ma, Z. Wang, Z. Zhao, H. Chen, K. Jiang, Y. Zhang, H. Yang, F. Zhou, X. Dong, S. L. Johnson, M. J. Graf, J. Hu, H.-J. Gao, and Z. Zhao, “Evidence of a hidden flux phase in the topological kagome metal  $CsV_3Sb_5$ ,” arXiv:2107.10714 (2021).
  - [23] Y. Hu, S. Yamane, G. Mattoni, K. Yada, K. Obata, Y. Li, Y. Yao, Z. Wang, J. Wang, C. Farhang, J. Xia, Y. Maeno, and S. Yonezawa, “Time-reversal symmetry breaking in charge density wave of  $CsV_3Sb_5$  detected by polar Kerr effect,” arXiv:2208.08036 (2022).
  - [24] C. Mielke III, D. Das, J. X. Yin, H. Liu, R. Gupta, Y. X. Jiang, M. Medarde, X. Wu, H. C. Lei, J. Chang, P. Dai, Q. Si, H. Miao, R. Thomale, T. Neupert, Y. Shi, R. Khasanov, M. Z. Hasan, H. Luetkens, and Z. Guguchia, “Time-reversal symmetry-breaking charge order in a kagome superconductor,” *Nature* **602**, 245 (2022).
  - [25] R. Khasanov, D. Das, R. Gupta, C. Mielke, M. Elender, Q. Yin, Z. Tu, C. Gong, H. Lei, E. T. Ritz, R. M. Fernandes, T. Birol, Z. Guguchia, and H. Luetkens, “Time-reversal symmetry broken by charge order in  $CsV_3Sb_5$ ,” *Phys. Rev. Res.* **4**, 023244 (2022).
  - [26] L. Nie, K. Sun, W. Ma, D. Song, L. Zheng, Z. Liang, P. Wu, F. Yu, J. Li, M. Shan, D. Zhao, S. Li, B. Kang, Z. Wu, Y. Zhou, K. Liu, Z. Xiang, J. Ying, Z. Wang, T. Wu, and X. Chen, “Charge-density-wave-driven electronic nematicity in a kagome superconductor,” *Nature*

- 604**, 59 (2022).
- [27] H. Li, H. Zhao, B. R. Ortiz, T. Park, M. Ye, L. Balents, Z. Wang, S. D. Wilson, and I. Zeljkovic, "Rotation symmetry breaking in the normal state of a kagome superconductor  $KV_3Sb_5$ ," *Nat. Phys.* **18**, 265 (2022).
- [28] Y. Xu, Z. Ni, Y. Liu, B. R. Ortiz, Q. Deng, S. D. Wilson, B. Yan, L. Balents, and L. Wu, "Three-state nematicity and magneto-optical Kerr effect in the charge density waves in kagome superconductors," *Nat. Phys.* **18**, 1470 (2022).
- [29] Z. Guguchia, C. Mielke, D. Das, R. Gupta, J.-X. Yin, H. Liu, Q. Yin, M. H. Christensen, Z. Tu, C. Gong, N. Shumiya, M. S. Hossain, T. Gamsakhurdashvili, M. Elender, P. Dai, A. Amato, Y. Shi, H. C. Lei, R. M. Fernandes, M. Z. Hasan, H. Luetkens, and R. Khasanov, "Tunable unconventional kagome superconductivity in charge ordered  $RbV_3Sb_5$  and  $KV_3Sb_5$ ," *Nature Commun.* **14**, 153 (2023).
- [30] R. Gupta, D. Das, C. H. Mielke III, Z. Guguchia, T. Shiroka, C. Baines, M. Bartkowiak, H. Luetkens, R. Khasanov, Q. Yin, Z. Tu, C. Gong, and H. Lei, "Microscopic evidence for anisotropic multigap superconductivity in the  $CsV_3Sb_5$  kagome superconductor," *npj Quant. Mater.* **7**, 49 (2022).
- [31] R. Gupta, D. Das, C. Mielke, E. T. Ritz, F. Hotz, Q. Yin, Z. Tu, C. Gong, H. Lei, T. Birol, R. M. Fernandes, Z. Guguchia, H. Luetkens, and R. Khasanov, "Two types of charge order with distinct interplay with superconductivity in the kagome material  $CsV_3Sb_5$ ," *Commun. Phys.* **5**, 232 (2022).
- [32] D. Weiyin, N. Zhiyong, L. Shuaishuai, Y. Fanghang, R. O. Brenden, Y. Lichang, S. Hang, D. Feng, W. An, C. Ye, L. Xin, Y. Jianjun, D. W. Stephen, C. Xianhui, S. Yu, and Y. Huiqiu, "Nodeless superconductivity in the kagome metal  $CsV_3Sb_5$ ," *Sci. China: Phys. Mech. Astron.* **64**, 107462 (2021).
- [33] Z. Shan, P. K. Biswas, S. K. Ghosh, T. Tula, A. D. Hillier, D. Adroja, S. Cottrell, G.-H. Cao, Y. Liu, X. Xu, Y. Song, H. Yuan, and M. Smidman, "Muon spin relaxation study of the layered kagome superconductor  $CsV_3Sb_5$ ," *Phys. Rev. Res.* **4**, 033145 (2022).
- [34] K. Roppongi, M. and Ishihara, Y. Tanaka, K. Ogawa, K. Okada, S. Liu, K. Mukasa, Y. Mizukami, Y. Uwatoko, R. Grasset, M. Konczykowski, B. R. Ortiz, S. D. Wilson, K. Hashimoto, and T. Shibauchi, "Bulk evidence of anisotropic s-wave pairing with no sign change in the kagome superconductor  $CsV_3Sb_5$ ," *Nat. Commun.* **14**, 667 (2023).
- [35] C. Mu, Q. Yin, Z. Tu, C. Gong, H. Lei, Z. Li, and J. Luo, "S-wave superconductivity in kagome metal  $CsV_3Sb_5$  revealed by  $^{121/123}Sb$  NQR and  $^{51}V$  NMR measurements," *Chin. Phys. Lett.* **38**, 077402 (2021).
- [36] W. Zhang, X. Liu, L. Wang, C. W. Tsang, Z. Wang, S. T. Lam, W. Wang, J. Xie, X. Zhou, Y. Zhao, S. Wang, J. Tallon, K. T. Lai, and S. K. Goh, "Nodeless superconductivity in kagome metal  $CsV_3Sb_5$  with and without time reversal symmetry breaking," *Nano Lett.* **23**, 872 (2023).
- [37] B. R. Ortiz, S. M. Teicher, L. Kautzsch, P. M. Sarte, N. Ratcliff, J. Harter, J. P. Ruff, R. Seshadri, and S. D. Wilson, "Fermi surface mapping and the nature of charge-density-wave order in the kagome superconductor  $CsV_3Sb_5$ ," *Phys. Rev. X* **11**, 041030 (2021).
- [38] H.-S. Xu, Y.-J. Yan, R. Yin, W. Xia, S. Fang, Z. Chen, Y. Li, W. Yang, Y. Guo, and D.-L. Feng, "Multiband superconductivity with sign-preserving order parameter in kagome superconductor  $CsV_3Sb_5$ ," *Phys. Rev. Lett.* **127**, 187004 (2021).
- [39] H. Luo, Q. Gao, H. Liu, Y. Gu, D. Wu, C. Yi, J. Jia, S. Wu, X. Luo, Y. Xu, L. Zhao, Q. Wang, H. Mao, G. Liu, Z. Zhu, Y. Shi, K. Jiang, J. Hu, Z. Xu, and X. J. Zhou, "Electronic nature of charge density wave and electron-phonon coupling in kagome superconductor  $KV_3Sb_5$ ," *Nat. Commun.* **13**, 273 (2022).
- [40] Y. Hu, X. Wu, B. R. Ortiz, X. Han, N. C. Plumb, S. D. Wilson, A. P. Schnyder, and M. Shi, "Coexistence of trihexagonal and star-of-david pattern in the charge density wave of the kagome superconductor  $AV_3Sb_5$ ," *Phys. Rev. B* **106**, L241106 (2022).
- [41] R. Chapai, M. Leroux, V. Oliviero, D. Vignolles, N. Bruyant, M. P. Smylie, D. Y. Chung, M. G. Kanatzidis, W.-K. Kwok, J. F. Mitchell, and U. Welp, "Magnetic breakdown and topology in the kagome superconductor  $CsV_3Sb_5$  under high magnetic field," *Phys. Rev. Lett.* **130**, 126401 (2023).
- [42] Y. Fu, N. Zhao, Z. Chen, Q. Yin, Z. Tu, C. Gong, C. Xi, X. Zhu, Y. Sun, K. Liu, and H. Lei, "Quantum transport evidence of topological band structures of kagome superconductor  $CsV_3Sb_5$ ," *Phys. Rev. Lett.* **127**, 207002 (2021).
- [43] F. H. Yu, T. Wu, Z. Y. Wang, B. Lei, W. Z. Zhuo, J. J. Ying, and X. H. Chen, "Concurrence of anomalous hall effect and charge density wave in a superconducting topological kagome metal," *Phys. Rev. B* **104**, L041103 (2021).
- [44] K. Shrestha, R. Chapai, B. K. Pokharel, D. Miertschin, T. Nguyen, X. Zhou, D. Y. Chung, M. G. Kanatzidis, J. F. Mitchell, U. Welp, D. Popović, D. E. Graf, B. Lorenz, and W. K. Kwok, "Nontrivial Fermi surface topology of the kagome superconductor  $CsV_3Sb_5$  probed by de Haas-van Alphen oscillations," *Phys. Rev. B* **105**, 024508 (2022).
- [45] X. Huang, C. Guo, C. Putzke, M. Gutierrez-Amigo, Y. Sun, M. G. Vergniory, I. Errea, D. Chen, C. Felser, and P. J. W. Moll, "Three-dimensional fermi surfaces from charge order in layered  $CsV_3Sb_5$ ," *Phys. Rev. B* **106**, 064510 (2022).
- [46] D. Chen, B. He, M. Yao, Y. Pan, H. Lin, W. Schnelle, Y. Sun, J. Gooth, L. Taillefer, and C. Felser, "Anomalous thermoelectric effects and quantum oscillations in the kagome metal  $CsV_3Sb_5$ ," *Phys. Rev. B* **105**, L201109 (2022).
- [47] Y. Gan, W. Xia, L. Zhang, K. Yang, X. Mi, A. Wang, Y. Chai, Y. Guo, X. Zhou, and M. He, "Magnetoseebeck effect and ambipolar Nernst effect in the  $CsV_3Sb_5$  superconductor," *Phys. Rev. B* **104**, L180508 (2021).
- [48] S.-Y. Yang, Y. Wang, B. R. Ortiz, D. Liu, J. Gayles, E. Derunova, R. Gonzalez-Hernandez, L. Šmejkal, Y. Chen, S. S. P. Parkin, S. D. Wilson, E. S. Toberer, T. McQueen, and M. N. Ali, "Giant, unconventional anomalous Hall effect in the metallic frustrated magnet candidate,  $KV_3Sb_5$ ," *Sci. Adv.* **6**, eabb6003 (2020).
- [49] L. Wang, W. Zhang, Z. Wang, T. F. Poon, W. Wang, C. W. Tsang, J. Xie, X. Zhou, Y. Zhao, S. Wang, K. T. Lai, and S. K. Goh, "Anomalous hall effect and two-dimensional fermi surfaces in the charge-density-wave

- state of kagome metal  $\text{RbV}_3\text{Sb}_5$ ,” *J. Phys. Mater.* **6**, 02LT01 (2023).
- [50] K. Shrestha, M. Shi, T. Nguyen, D. Miertschin, K. Fan, L. Deng, D. E. Graf, X. Chen, and C.-W. Chu, “Fermi surface mapping of the kagome superconductor  $\text{rbv}_3\text{sb}_5$  using de haas-van alphen oscillations,” *Phys. Rev. B* **107**, 075120 (2023).
- [51] J. Xie, X. Liu, W. Zhang, S. M. Wong, X. Zhou, Y. Zhao, S. Wang, K. T. Lai, and S. K. Goh, “Fragile pressure-induced magnetism in  $\text{FeSe}$  superconductors with a thickness reduction,” *Nano Lett.* **21**, 9310 (2021).
- [52] C.-h. Ku, X. Liu, J. Xie, W. Zhang, S. T. Lam, Y. Chen, X. Zhou, Y. Zhao, S. Wang, S. Yang, K. T. Lai, and S. K. Goh, “Patterned diamond anvils prepared via laser writing for electrical transport measurements of thin quantum materials under pressure,” *Rev. Sci. Instrum.* **93**, 083912 (2022).
- [53] W. Zhang, L. Wang, C. W. Tsang, X. Liu, J. Xie, W. C. Yu, K. T. Lai, and S. K. Goh, “Emergence of large quantum oscillation frequencies in thin flakes of a kagome superconductor  $\text{CsV}_3\text{Sb}_5$ ,” *Phys. Rev. B* **106**, 195103 (2022).
- [54] H. Tan, Y. Liu, Z. Wang, and B. Yan, “Charge density waves and electronic properties of superconducting kagome metals,” *Phys. Rev. Lett.* **127**, 046401 (2021).